PERGAMON

Available online at www.sciencedirect.com

SCIENCE DIRECT®

Polyhedron 22 (2003) 805–810

POLYHEDRON

www.elsevier.com/locate/poly

Insertion of sulfur dioxide into metal–carbon bonds of chloro(methyl)palladium complexes

Kelin Li [a], Ilia A. Guzei [b], James Darkwa [a,*]

[a] Department of Chemistry, University of the Western Cape, Private Bag X17, Bellville 7535, South Africa
[b] Department of Chemistry, University of Wisconsin-Madison, 1101 University Avenue, Madison, WI 53706, USA

Received 7 October 2002; accepted 21 November 2002

Abstract

Five chloro(methyl)palladium complexes (L–L)Pd(Me)Cl have been shown to react with SO_2 in solution to form S-sulfinato complexes of the formula (L–L)Pd(SO_2Me)Cl (L–L = dippf = 1,1′-bis(diisopropylphosphino)ferrocene (**2**), dppf = bis(diphenylphosphino)ferrocene (**3**), dppe = 1,1′-bis(diphenylphosphino)ethane (**4**), COD (**5**) and (3,5-di^{t}Bupz)$_2$ (**6**)). Compounds **5** and **6** are unstable in solution and slowly decompose. Representative crystal structures of (dippf)Pd(Me)Cl (**1**) and (dppf)Pd(SO_2Me)Cl (**3**) are reported.

Keywords: Palladium complexes; Insertion; Sulfur dioxide; Crystal structures

1. Introduction

There are three main reaction types between metal complexes and sulfur dioxide. The first type involves sulfur dioxide binding to the metal center [1]. The second type is sulfur dioxide binding to a ligand in the metal complex [2] and the third is insertion of sulfur dioxide into a metal–hydrogen [1b], metal–carbon [3] or metal–metal bonds [4]. Insertion into a metal–carbon bond is observed predominantly for the late transition metals, notably Group 8 metals. The first report on the SO_2 insertion into a metal–carbon bond was by Bibler and Wojcicki for the Fe–C bond in (η^5-C_5H_5)Fe-(CO)$_2$(R) to form the S-sulfinato products (η^5-C_5H_5)Fe(CO)$_2$(SO_2R) (R=CH_3, CH_2CH_3) [5]. Since then a number of S-sulfinato metal complexes have been prepared by this route [3,6]. Insertion of SO_2 into a Pd–C bond reported by Turner and Felkin in 1976 produces similar S-sulfinato products (η^5-C_5H_5)Pd(PPh_3)(SO_2R) (R=Me, Ph) [7]. The most recent reports by Jones and coworkers on reactions between Cp*Ir(PMe_3)(Me)Cl (Cp* = η^5-$C_5(CH_3)_5$) [8] and (dcpe)Pt(Me)Cl (dcpe = $Cy_2PC_2H_4PCy_2$) [9] and SO_2 reveal the instability of their insertion products. Whereas the reaction of SO_2 with chloro(methyl)iridium complex led to several unidentified insertion compounds [8], the chloro(methyl)platinum complex did not form the expected product, (dcpe)Pt(SO_2Me)Cl, and instead (dcpe)Pt(SO_2Me)Me and (dcpe)$PtCl_2$ were formed [9]. The lack of a single insertion product for Cp*Ir(PMe_3)-(Me)Cl is attributed to the instability of Cp*Ir(PMe_3)-(Me)Cl, which disproportionates to Cp*Ir(PMe_3)(Me)$_2$ and Cp*Ir(PMe_3)Cl_2 [8]. On the other hand, (dcpe)Pt-(Me)Cl does not disproportionate but the expected SO_2 insertion product, (dcpe)Pt(SO_2Me)Cl, is believed to be unstable; leading to the disproportionation products, (dcpe)Pt(SO_2Me)Me and (dcpe)$PtCl_2$ [9].

We have investigated the stability of SO_2 insertion products of five chloro(methyl)palladium complexes with different ligands, to test how ancillary ligands affect the stability of insertion products. The results of this study are reported in this paper.

2. Experimental

All manipulations were performed under a dry nitrogen atmosphere using standard Schlenk techniques. NMR spectra were recorded on a Gemini 2000 instru-

* Corresponding author

0277-5387/02/$ - see front matter © 2002 Published by Elsevier Science Ltd.
doi:10.1016/S0277-5387(02)01377-3

ment (^{1}H at 200 MHz, ^{13}C{^{1}H} at 50.3 MHz). The chemical shifts are reported in δ (ppm) referenced to residual protons and ^{13}C signals of deuterated $CHCl_3$ as internal standard. (COD)Pd(Me)Cl [10], (3,5-di^t-Bupz)$_2$Pd(Me)Cl [11], (dppf)Pd(Me)Cl [12], (dppe)Pd-(Me)Cl [12] were prepared by literature methods. Sulfur dioxide (99.9+%) was obtained from Aldrich and used as received. Elemental analyses were performed in-house at the Department of Chemistry, University of the Western Cape.

2.1. (dippf)Pd(Me)Cl (1)

This compound was prepared by a similar procedure as reported for (dppf)Pd(Me)Cl [11]. Yield: 51%. *Anal*. Calc. for $C_{23}H_{39}ClFeP_2Pd$: C, 48.03; H, 6.83. Found: C, 47.90; H, 6.55%. ^{1}H NMR ($CDCl_3$): δ 4.37 (s, br, 8H, C_5H_4); 2.67 (m, 2H, ^{i}Pr); 2.41 (m, 2H, ^{i}Pr); 1.48 (dd, 6H, ^{i}Pr, $^2J_{HH} = 15.9$, $^3J_{PH} = 7.3$ Hz); 1.20 (m, 18H, ^{i}Pr); 0.90 (dd, 3H, Pd–Me, $^3J_{PH} = 6.9$, $^3J_{PH} = 2.9$ Hz). ^{13}C{^{1}H} NMR ($CDCl_3$): δ 73.3, 73.2, 72.9, 72.8, 71.0, 70.9, 70.6, 70.5, 26.0, 25.5, 25.4, 25.2, 20.9, 20.7, 19.6, 19.5, 19.4, 19.3, 8.5, 8.4, 6.5, 6.4.

2.2. (dippf)Pd(SO$_2$Me)Cl (2)

Sulfur dioxide was bubbled through a CH_2Cl_2 (15 ml) solution of (dippf)Pd(Me)Cl (0.20 g, mmol) for 15 min. The yellow solution turned red. Addition of C_6H_{14}, saturated with SO_2, gave analytically pure crystalline (dippf)Pd(SO_2Me)Cl. Yield: 0.14 g, 65%. *Anal*. Calc. for $C_{23}H_{39}ClFeO_2P_2PdS$: C, 43.21; H, 6.15. Found: C, 42.85; H, 6.20%. ^{1}H NMR ($CDCl_3$): δ 4.55 (s, br, 8H, C_5H_4); 3.52 (m, 2H, ^{i}Pr); 3.13 (s, 3H, –SO_2Me); 2.95 (m, 2H, ^{i}Pr); 1.64 (m, 2H, ^{i}Pr); 1.05–1.25 (m, 2H, ^{i}Pr). ^{13}C{^{1}H} NMR ($CDCl_3$): δ 73.5, 73.3, 73.0, 72.9, 71.2, 71.0, 70.8, 70.6, 31.0, 26.2, 25.7, 25.4, 25.2, 20.9, 20.7, 19.6, 19.5, 19.3, 8.5, 8.4, 6.5, 6.4.

A similar procedure as used for complex **2** was followed to prepare complexes **3**, **4** and **5**.

2.3. (dppf)Pd(SO$_2$Me)Cl (3)

Single crystals suitable for X-ray analysis were obtained by layering a CH_2Cl_2 solution of **3** with SO_2 saturated C_6H_{14} at −15 °C. Yield: 69%. *Anal*. Calc. for $C_{35}H_{31}ClFeO_2P_2PdS\cdot CH_2Cl_2$: C, 50.26; H, 3.87. Found: C, 50.40; H, 3.54%. ^{1}H NMR ($CDCl_3$): δ 7.82 (m, 4H, Ph); 7.39 (m, 6H, Ph); 4.70 (s, br, 2H, C_5H_4); 4.51 (s, br, 2H, C_5H_4); 4.25 (s, br, 2H, C_5H_4); 3.56 (s, br, 2H, C_5H_4); 2.98 (s, 3H, –SO_2Me). ^{13}C{^{1}H} NMR ($CDCl_3$): δ 134.7, 131.5, 131.0, 75.3, 74.1, 73.3, 71.6, 31.7.

2.4. (dppe)Pd(SO$_2$Me)Cl (4)

Yield: 60%. *Anal*. Calc. for $C_{27}H_{27}ClO_2P_2PdS$: C, 52.36; H, 4.39. Found: C, 52.10; H, 4.50%. ^{1}H NMR ($CDCl_3$): δ 7.80 (m, 8H, Ph); 7.53 (m, 12H, Ph); 2.74 (s, 3H, –SO_2Me); 2.61 (s, br, 2H, CH_2); 2.10 (s, br, 2H, CH_2). ^{13}C{^{1}H} NMR ($CDCl_3$): δ 133.7, 133.4, 132.9, 129.6, 129.3, 127.0, 125.9, 40.2, 28.6, 28.3, 27.5, 27.3.

2.5. (3,5-di^{t}Bupz)$_2$Pd(SO$_2$Me)Cl (5)

Yield: 55%. *Anal*. Calc. for $C_{23}H_{43}ClN_4O_2P_2PdS$: C, 47.50; H, 7.45; N, 9.63. Found: C, 47.20; H, 7.10; N, 10.05%. ^{1}H NMR ($CDCl_3$): δ 6.06 (s, 2H, pz); 3.12 (s, 3H, –SO_2Me); 1.37 (s, 36H, ^{t}Bu). ^{13}C{^{1}H} NMR ($CDCl_3$): δ 146.8, 132.5, 122.5, 43.8, 40.6, 16.8, 14.9.

2.6. (COD)Pd(SO$_2$Me)Cl (6)

A slow stream of SO_2 was bubbled through a CH_2Cl_2 (15 ml) solution of (COD)Pd(Me)Cl (0.30 g, 1.15 mmol) for 15 min. The colourless solution turned yellow and the reaction mixture was kept under SO_2 pressure and stirred for 18 h. Upon addition of SO_2 saturated C_6H_{14}, the solution gradually deposited yellow microcrystalline (COD)Pd(SO_2Me)Cl. Yield: 0.26 g, 70%. *Anal*. Calc. for $C_9H_{15}ClO_2PdS$: C, 32.80; H, 4.59. Found: 33.25; H, 4.41%. ^{1}H NMR ($CDCl_3$): δ 6.18 (s, br, 2H, COD); 5.97 (s, br, 2H, COD); 3.22 (s, 3H, SO_2Me); 2.89 (m, 4H, COD); 2.71 (m, 4H, COD). ^{13}C{^{1}H} NMR ($CDCl_3$): δ 126.3, 118.7, 30.6, 28.5, 26.0.

2.7. X-ray structural determination for 1 and 3

Crystal evaluation and data collection were performed on a Bruker CCD-1000 diffractometer with Mo Kα ($\lambda = 0.71073$ Å) radiation and the diffractometer to crystal distance of 4.9 cm (Table 1). The initial cell constants were obtained from three series of ω scans at different starting angles. The reflections were successfully indexed by an automated indexing routine built in the SMART program. The absorption correction was based on fitting a function to the empirical transmission surface as sampled by multiple equivalent measurements [13]. The structures were solved by direct methods and refined by least-squares techniques using SHELXTL program [14]. All non-hydrogen atoms were refined with anisotropic displacement coefficients. All hydrogen atoms were included in the structure factor calculation at idealized positions and were allowed to ride on the neighbouring atoms with relative isotropic displacement coefficients. Complex **1** occupies a crystallographic twofold axis; consequently, the chloride and methyl groups are equally disordered over the twofold axis. There was also one severely disordered molecule of CH_2Cl_2 present in the asymmetric unit of **3**. A sig-

Table 1
Crystal data and structure refinement for complexes **1** and **3**

Empirical formula	$C_{23}H_{39}ClFeP_2Pd$	$C_{35}H_{31}ClFeO_2P_2PdS\cdot CH_2Cl_2$
Formula weight	575.18	860.22
Temperature (K)	100(2)	173(2)
Wavelength (Å)	0.71073	0.71073
Crystal system	orthorhombic	monoclinic
Space group	*Pnna*	$P2_1/c$
a (Å)	15.8149(7)	9.5395(10)
b (Å)	17.0533(8)	20.568(2)
c (Å)	8.9562(4)	18.9395(17)
α (°)	90	90
β (°)	90	92.590(2)
γ (°)	90	90
Volume (Å^3)	2415.45(19)	3712.3(6)
Z	4	4
D_{calc} (Mg m^{-3})	1.582	1.539
Absorption coefficient (mm^{-1})	1.596	1.264
$F(000)$	1184	1736
Crystal size (mm)	0.40 × 0.20 × 0.20	0.40 × 0.31 × 0.15
θ Range (°)	2.57–26.38	1.46–26.37
Index ranges	$-19 \le h \le 19$, $-21 \le k \le 21$, $-11 \le l \le 11$	$-11 \le h \le 11$, $0 \le k \le 25$, $0 \le l \le 23$
Reflections collected	17 546	23 917
Independent reflections	2463 [$R_{int} = 0.0299$]	7408 [$R_{int} = 0.0388$]
Completeness to $\theta = 26.37°$	99.6%	97.8%
Absorption correction	empirical with SADABS	empirical with SADABS
Max./min. transmission	0.7408, 0.5677	0.8330, 0.6317
Refinement method	full-matrix least-squares on F^2	full-matrix least-squares on F^2
Data/restraints/parameters	2463/2/137	7408/0/393
Final R indices [$I > 2\sigma(I)$]	$R_1 = 0.0325$, $wR_2 = 0.0960$	$R_1 = 0.0361$, $wR_2 = 0.0900$
R indices (all data)	$R_1 = 0.0357$, $wR_2 = 0.0988$	$R_1 = 0.0528$, $wR_2 = 0.0953$
Goodness-of-fit on F^2	1.005	1.049
Largest difference peak and hole (e Å^{-3})	0.678 and −0.438	1.306 and −0.498

nificant amount of time was invested in refining the disordered molecule. Bond length restraints were applied to model that molecule but the resulting isotropic displacement coefficients suggested the molecules were mobile. In addition, the refinement was computationally unstable. Option SQUEEZE of programme PLATON [15] was used to correct the diffraction data for diffuse scattering effects and to identify the solvate molecule.

3. Results and discussions

3.1. Synthesis of (dippf)PdMeCl (1)

The reaction of (COD)PdMeCl with 1 equiv. of 1,1′-bis(diisopropylphosphino)ferrocene (dippf) in CH_2Cl_2 at room temperature for 8 h afforded (dippf)PdMeCl as a yellow solid in only moderate yield. Complex **1** is very stable in both solution and solid-state. The methyl protons in **1** appear as doublet of a doublet at 0.90 ppm, the result of coupling with the two phosphorus atoms. The solid-state structure of **1** was determined by X-ray crystallography and shown in Fig. 1 with selected bond distances and angles in Table 2. The structure of **1** has a twofold crystallographic axis that passes through the Pd and Fe atoms. This results in an 50:50 occupancy of the methyl and Cl groups. The Pd is at the centre of a distorted square-planar geometry. The largest deviation from square-planarity is found in the P–Pd–P bite angle of 104.74(3)°, which is larger than bite angles in other (dippf)Pd complexes ((dippf)Pd(SC_6H_5)$_2$ (101.09(2)°) [16], (dippf)Pd(SC_6H_4S-*o*) (102.44(3)°),

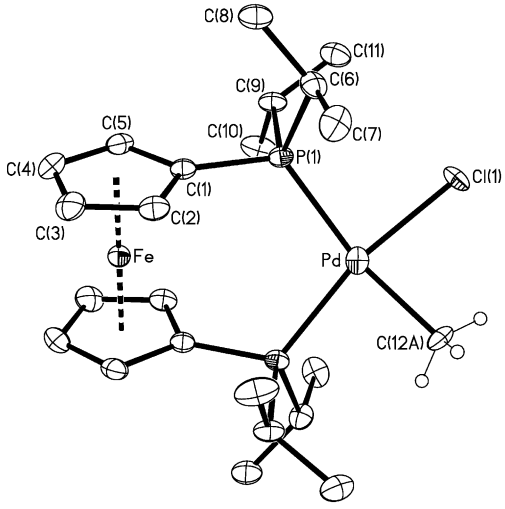

Fig. 1. ORTEP diagram of (dippf)Pd(Me)Cl.

Table 2
Selected bond lengths (Å) and angles (°) for complex **1**

Bond lengths			
Pd–P(1)	2.3339(7)	Pd–C(12)	2.051(2)
Pd–Cl(1)	2.3398(11)	P(1)–C(1)	1.813(3)
Bond angles			
P(1)–Pd–Cl(1)	87.28(8)	P(1)–Pd–P(1)#1	104.74(3)
C(12)#1–Pd–P(1)	167.9(5)	C(12)–Pd–Cl(1)#1	82.7(4)
P(1)–Pd–Cl(1)#1	167.53(9)	C(12)–Pd–P(1)	85.7(5)

(dippf)Pd(SC_6H_3MeS-*o*) (101.88(3)°) [17]). Similar to the Pd–P distances in (dippf)Pd(SC_6H_5)$_2$ (2.3303(6) and 2.3463(7) Å) [16], (dippf)Pd(SC_6H_4S-*o*) (2.3364(10) and 2.3433(8) Å) and (dippf)Pd(SC_6H_3MeS-*o*) (2.3291(9) and 2.3329(8) Å) [17], the Pd–P distance in **1** (2.3339(7) Å) is slightly longer than 'normal' Pd–P bond (2.29(5) Å) in average Pd–P bond distances in 2422 such distances in complexes in the Cambridge Structural Database (CSD) [18]. There is no *trans* effect on the Pd–P distances from the Cl and Me groups bonded to Pd in **1**. The Pd–Cl (2.3338(11) Å) and Pd–C (2.051(2) Å) in **1** are similar in length to those found in (σ^2-*N*,*N*′-^{i}Pr–DIP)Pd(Me)Cl (Pd–Cl (2.324(3) Å and Pd–C (2.01(1) Å) and [(terpy)Pd(Me)]$^+$ [Pd–C (2.041(12) Å] [10b].

3.2. Reactions with sulfur dioxide

All the chloro(methyl)palladium complexes readily reacted with SO_2 (Eq. (1)).

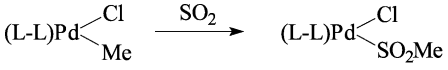

(1)

(L-L = dppf, dippf, dppe, COD, 3,5-di^{t}Bupz)

The complexes with phosphorous and nitrogen ligands changed from yellow to red, whilst the COD complex changed from colourless to yellow. Thus colour changes were a clear indication of reaction. From the ^{1}H NMR spectra, it was easy to establish insertion of SO_2 into the Pd–C bond. This involved downfield chemical shifts (Table 3). Insertion of small molecules into Pd–C bonds as in (dppf)Pd(C(O)Me)Cl and (dppe)Pd(C(O)Me)Cl [12] shifts methyl proton resonance downfield by more than 1.0 ppm from the peaks of the complexes prior to insertion. The changes in chemical shifts of the CO insertion products, (dppf)Pd(C(O)Me)Cl and (dppe)Pd(C(O)Me)Cl, are 1.20 and 1.41 ppm, respectively. These chemical shift changes are smaller than those found in the SO_2 insertion products (dppf)Pd(SO_2)Me)Cl (2.19 ppm) and (dppe)Pd(SO_2)Me)Cl (1.98 ppm). Nevertheless, both CO and SO_2 insertion products represent electron-withdrawal from the methyl group after insertion. A confirmation of SO_2 insertion into the Pd–C bond is provided by the X-ray structure of (dppf)Pd(SO_2Me)Cl (Fig. 2). The differences in chemical shifts of the methyl protons of the diphosphino complexes prior to SO_2 insertion and after ($\delta_2-\delta_1$ in Table 3) can be seen as a measure of the extent of back bonding. For example ($\delta_2-\delta_1$) for the dippf complex is 2.23 ppm whilst the dppf and dppe complexes have ($\delta_2-\delta_1$) values of 2.19 and 1.98 ppm, respectively. Thus the back bonding in the dippf complex is more extensive.

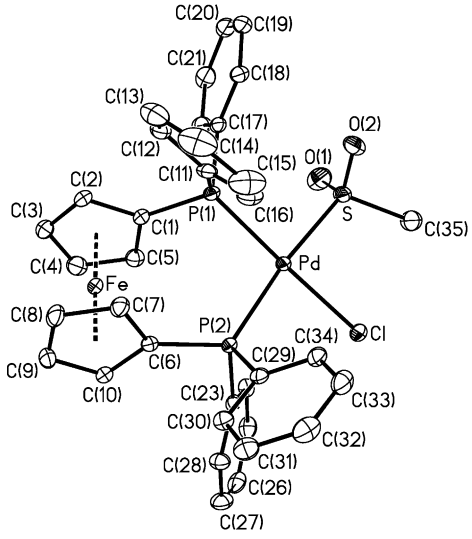

Fig. 2. ORTEP diagram of (dppf)Pd(SO_2Me)Cl.

When a slow stream of nitrogen was bubble through a $CDCl_3$ solution of **5**, the ^{1}H NMR spectrum showed that the solution was nearly 1:1 mixture of (3,5-di^{t}Bupz)$_2$Pd(Me)Cl and (3,5-di^{t}Bupz)$_2$Pd(SO_2Me)Cl and a small amount of an unidentified product; indicating some reversibility of the SO_2 insertion.

The solid-state structure of complex **3** is shown in Fig. 2 and depicts the insertion of SO_2 into the Pd–C bond.

Table 3
^{1}H NMR of methyl chemical shifts of pre-insertion compounds and insertion products

Complex	δ_1 (ppm)	Insertion product	δ_2 (ppm)	$\Delta(\delta_2-\delta_1)$ (ppm)
(dppf)PdMeCl	0.79	(dppf)Pd(SO_2Me)Cl	2.98	2.19
(dippf)PdMeCl	0.90	(dippf)Pd(SO_2Me)Cl	3.13	2.23
(dppe)PdMeCl	0.76	(dppe)Pd(SO_2Me)Cl	2.74	1.98
(3,5-di^{t}Bupz)$_2$PdMeCl	−0.14	(3,5-di^{t}Bupz)$_2$Pd(SO_2Me)Cl	3.12	3.26
(COD)PdMeCl	1.17	(COD)Pd(SO_2Me)Cl	3.22	2.05

Table 4
Selected bond lengths (Å) and angles (°) for complex **3**

Bond lengths			
Pd–P(1)	2.3104(7)	Pd–S	2.3262(9)
Pd–Cl	2.3528(7)	Pd–P(2)	2.3767(8)
S–C(35)	1.789(3)	S–O(1)	1.484(3)
P(1)–C(1)	1.800(3)	P(2)–C(6)	1.809(3)
S–O(2)	1.458(3)		
Bond angles			
P(1)–Pd–S	89.34(3)	P(1)–Pd–Cl	176.59(3)
S–Pd–Cl	89.91(3)	P(1)–Pd–P(2)	96.90(3)
S–Pd–P(2)	173.71(3)	Cl–Pd–P(2)	83.82(3)
C(35)–S–Pd	113.04(14)	O(1)–S–Pd	110.44(2)
O(2)–S–Pd	110.71(13)	O(2)–S–O(1)	115.47(8)

Table 4 contains selected bond distances and angles. The geometry around the Pd in **3** is distorted square-planar, with the *cis* angle ranging between 83.82(3)° and 96.90(3)°. The bite angle of the bidentate ligand is similar to that in (dppf)Pd(SC_6H_4S-*o*) (97.24°) [17], but slightly larger than the corresponding angle observed in (dppf)$PdCl_2$ (99.07°) [19]. Similarly, the average Pd–P (2.310 Å) and Pd–S (2.326 Å) distances in **3** are only slightly longer than the average Pd–P distance (2.29(5) Å) and the average Pd–S distance (2.30(3) Å) obtained by averaging 2422 and 340 corresponding distances, respectively reported to the CSD [18]. Hence, the insertion of SO_2 into the Pd–C bond does not seem to affect the Pd–P and Pd–S distances considerably.

The reaction of (COD)Pd(Me)Cl with SO_2 was much slower than those of the phosphine and pyrazole complexes. Complete conversion of (COD)Pd(Me)Cl to (COD)Pd(SO_2Me)Cl took 18 h (Table 5). The (P–P)Pd(SO_2Me)Cl products (**2**–**4**) were stable in solution for indefinite periods as evidenced by the slow crystallization of **2** from 1:1 mixture of CH_2Cl_2/hexane over several days. Complexes **2**–**4** decomposed when heated in the solid-state at 80 °C, without the de-insertion of SO_2, to unidentified products. However, both (3,5-di^{t}Bupz)$_2$Pd(SO_2Me)Cl (**5**) and (COD)Pd(SO_2Me)Cl (**6**) were unstable in solution over long periods.

Table 5
Effect of time on the SO_2 insertion reaction and product stability of (COD)Pd(SO_2Me)Cl

Time	^{1}H NMR ($CDCl_3$) (ppm)
0	5.90 (m, 2H, COD); 5.15 (m, 2H, COD); 2.62 (m, 4H, COD); 2.46 (m, 4H, COD); 1.17 (s, 3H, Pd–Me)
15 min	6.17 (m, 2H, COD); 5.96 (m, 2H, COD); 5.90 (m, 2H, COD); 5.15 (m, 2H, COD); 3.22 (s, 3H, SO_2Me); 2.75 (m, 4H, COD); 2.62 (m, 4H, COD); 2.46 (m, 4H, COD); 1.17 (s, 3H, Pd–Me)
18 h	6.18 (s, br, 2H, COD); 5.97 (s, br, 2H, COD); 3.22 (s, 3H, SO_2Me); 2.89 (m, 4H, COD); 2.71 (m, 4H, COD)
3 days	6.18 (s, br, 2H, COD); 6.06 (m, 2H, COD); 5.97 (s, br, 2H, COD); 5.60 (m, 2H, COD); 3.22 (s, 3H, –SO_2Me); 2.90 (m, 4H, COD); 2.88 (s, 3H, SO_2Me); 2.70 (m, 4H, COD)
11 days	6.06 (m, 2H, COD); 5.60 (m, 2H, COD); 2.90 (m, 4H, COD); 2.88 (s, 3H, SO_2Me); 2.70 (m, 4H, COD)

Wojcicki observed several years ago that SO_2 insertion into metal–carbon bond is electrophilic in nature [3a]. It is therefore conceivable that the stability of (P–P)Pd(SO_2Me)Cl compared to (3,5-di^{t}Bupz)$_2$Pd(SO_2Me)Cl and (COD)Pd(SO_2Me)Cl could be due to the presence of the more electron-donating diphosphino ligands. Both (3,5-di^{t}Bupz)$_2$Pd(SO_2Me)Cl and (COD)Pd(SO_2Me)Cl slowly decomposed in solution over several days. By monitoring the SO_2 reaction with ^{1}H NMR spectroscopy (Table 5), three new sets of peaks were found at 6.18, 5.96–5.97 and 3.22 ppm after 15 min in addition to (COD)Pd(Me)Cl peaks. The peaks of (COD)Pd(Me)Cl disappeared completely after 18 h, leaving only peaks of (COD)Pd(SO_2Me)Cl. After 3 days, a completely new set of peaks appeared at 6.03–6.10, 5.58–5.63, 2.89 ppm, in addition to reduced intensity peaks of (COD)Pd(SO_2Me)Cl. After 11 days, all the (COD)Pd(SO_2Me)Cl peaks had disappeared completely, a clear indication that (COD)Pd(SO_2Me)Cl is unstable in solution over a long period. The final decomposition product is a mixture of unidentifiable compounds, based on the ^{1}H NMR, but the decomposition does not lead to SO_2 desorption; hence the SO_2 insertion reaction is not reversible.

4. Conclusions

Insertion of SO_2 into Pd–C bond produces S-sulfinato palladium complexes in moderate yields. The SO_2 insertion with the complexes bearing diphosphino ancillary ligands appears to be more facile, which is in accord with the electrophilic nature of SO_2 insertion mechanism. The insertion products **5** and **6** showed signs of decomposition upon storage in solution, which was more pronounced for **6**. Decomposition of **5** was mainly due to SO_2 de-insertion, indicating reversibility of the insertion process in the absence of the reaction condition necessary to shift the equilibrium toward the insertion product.

5. Supplementary material

Crystallographic data for the structural analysis have been deposited with the Cambridge Crystallographic Data Centre, CCDC Nos. 185331 and 158332. Copies of this information may be obtained free of charge from The Director, CCDC, 12 Union Road, Cambridge, CB2 1EZ, UK (fax: +44-1223-336033; e-mail: deposit@ccdc.cam.ac.uk or www: http://www.ccdc.cam.ac.uk).

Acknowledgements

This work was supported by the National Research Foundation (South Africa) and in part by the International Foundation for Science (IFS) (Sweden).

References

[1] (a) D.M.P. Mingos, R.W.W. Wardle, J. Chem. Soc., Dalton Trans. (1986) 73;
(b) G.J. Kubas, R.R. Ryan, Polyhedron 5 (1986) 473;
(c) W.A. Schnek, Angew. Chem., Int. Ed. Engl. 98 (1987) 109.
[2] J. Darkwa, R.M. Moutloali, T. Nyokong, J. Organomet. Chem. 564 (1998) 37 (and references therein).
[3] (a) A. Wojcicki, Adv. Organomet. Chem. 12 (1974) 31;
(b) A. Wojcicki, Acc. Chem. Res. 4 (1971) 344;
(c) M.F. Joseph, M.C. Baird, Inorg. Chim. Acta 95 (1985) 229;
(d) C.W. Fong, W. Kitching, J. Organomet. Chem. 22 (1970) 95.
[4] D.H. Farrar, R.R. Gukathasan, J. Chem. Soc., Dalton Trans. (1989) 557.
[5] (a) J.P. Bibler, A. Wojcicki, J. Am. Chem. Soc. 86 (1964) 505;
(b) J.P. Bibler, A. Wojcicki, J. Am. Chem. Soc. 88 (1966) 4862.
[6] W. Kitching, C.W. Fong, Organomet. Chem. Rev., A 5 (1970) 281.
[7] G.K. Turner, H. Felkin, J. Organomet. Chem. 121 (1976) C29.
[8] L. Lefort, R.J. Lachicotte, W.D. Jones, Organometallics 17 (1998) 1420.
[9] M.S. Morton, R.J. Lachicotte, D.A. Vicic, W.D. Jones, Organometallics 18 (1999) 227.
[10] (a) P.W.N.M. van Leeuwen, C.F. Roobeek, Eur. Pat. Appl., 1990, 380,162.;
(b) R.E. Rulke, I.M. Han, C.J. Elsevier, K. Vrieze, P.W.N.M. van Leeuwen, C.F. Roobeek, M.C. Zoutberg, Y.F. Wang, C.H. Stam, Inorg. Chim. Acta 169 (1990) 5.
[11] K. Li, J. Darkwa, I.A. Guzei, S.F. Mapolie, J. Organomet. Chem. 600 (2002) 109.
[12] G.P.C. Dekker, C.J. Elsevier, K. Vrieze, P.W.N.M. van Leeuwen, Organometallics 11 (1992) 1598.
[13] R.H. Blessing, Acta Crystallogr., Sect. A 51 (1995) 33.
[14] All software and sources of the scattering factors are contained in the SHELXTL (Version 5.1) program library (G.M. Sheldrick, Bruker Analytical X-ray Systems, Madison, WI).
[15] A.L. Spek, Acta Crystallogr., Sect. A 46 (1990) 34.
[16] I.A. Guzei, L.L. Maisela, J. Darkwa, Acta Crystallogr., Sect. C 56 (2000) 564.
[17] L.L. Maisela, A.M. Crouch, J. Darkwa, I.A. Guzei, Polyhedron 20 (2001) 3189.
[18] F.H. Allen, O. Kennard, Chem. Des. Autom. News 8 (1993) 31.
[19] T. Hayashi, M. Konishi, Y. Kobori, M. Kumada, T. Higuchi, K. Hirotsu, J. Am. Chem. Soc. 106 (1984) 158.